Scattering in periodic systems: from resonances to band structure

1999 J. Phys. A: Math. Gen. 32 3357

(http://iopscience.iop.org/0305-4470/32/18/310)

J. Phys. A: Math. Gen. **32** (1999) 3357–3375. Printed in the UK PII: S0305-4470(99)99546-X

Scattering in periodic systems: from resonances to band structure

F Barra and P Gaspard

Center for Nonlinear Phenomena and Complex Systems, Université Libre de Bruxelles, Campus de la Plaine CP 231, B-1050 Brussels, Belgium

Received 23 November 1998, in final form 25 February 1999

Abstract. We report a study of the spectrum of scattering resonances in spatially extended open quantum systems. We consider the Schrödinger equation with a potential composed of n copies of a unit cell periodically arranged in a one-dimensional space and vanishing at large distances. We develop an asymptotic theory which explains the structure of the resonance spectrum. We also show that, in the limit of a large system, the leading scattering resonances converge to the allowed energy bands of the infinitely extended periodic system.

1. Introduction

Scattering systems are of great importance in physics and chemistry. In many experimental situations, the system is probed and studied by the scattering of a beam of particles. In such scattering experiments, the system properties can be obtained by the measurement of the differential or total cross sections. In many cases, the cross sections reveal a spectrum of resonances appearing around certain energies. The resonances are associated with metastable states for which the beam particle is transiently trapped inside the system for a time duration called the lifetime [1–7]. The spectrum of the scattering resonances can therefore be used to characterize the internal dynamics of the system. For instance, in mesoscopic opto-electronic devices, the scattering resonances give an estimation of the time of relaxation of the circuit after an optical excitation [8]. In chemical photodissociations, the scattering resonances provide the unimolecular reaction rates of the molecular system [9, 10]. In this context, many recent works have been devoted to the phenomenon of scattering on a classically chaotic system, notably, in the semiclassical limit [3, 11, 12]. However, these works have remained restricted to small systems with a few centres of collision localized in a limited spatial region.

Of growing interest is the scattering on spatially extended systems, for which an important question is to understand how the transport properties like conductance and diffusion are related to the spectrum of scattering resonances. In this paper, we consider the scattering on one-dimensional systems where the scatterer is composed of n copies of a unit cell periodically arranged (the system is spatially periodic in the strict sense when $n \to \infty$). A linear molecule or a crystal are examples of such systems in which the unit cell is composed of a single atom or of a group of atoms. Our purpose is to develop a general asymptotic theory to construct the spectrum of resonances for such spatially extended systems. We show that the resonance spectrum displays a remarkable structure which may be regular or irregular. This structure is in close connection with the energy bands of the infinite periodic system and it characterizes the dynamics of finite periodic systems in a similar way as the energy bands do

0305-4470/99/183357+19$19.50

for the corresponding infinite system. For instance, in the infinite-system limit, the dynamics can be summarized in the relation $v_b = \frac{1}{\hbar}\frac{\mathrm{d}E_n(q)}{\mathrm{d}q}$ between the group velocity of a wavepacket and the eigenenergies [13]. On the other hand, for a finite system, the dynamics is governed by the lifetimes of the scattering resonance spectrum. An important result is that we prove that the leading scattering resonances converge to the allowed energy bands in the infinite-system limit.

Moreover, we compare the properties of the lifetimes with those of the Wigner time delay function, which is a usual tool to obtain dynamical information about a scattering process. In particular, for systems where the transmission probability is a smooth and slowly varying function of the wavenumber there is an important lengthening of the quantum lifetimes near the edges of the energy bands. This lengthening is also observed in the Wigner time delay function. We also explore the behaviour of both the resonance spectrum and the Wigner time delay function as a function of the size of the system and of the energy of the scattered particle.

The plan of the paper is the following. In section 2, we summarize the relevant properties of the scattering resonances. In section 3, we show that the scattering resonances form a structure in the complex wavenumber plane for a finite periodic potential in one dimension. We give an analytic asymptotic expression for this structure and we compute the resonance lifetimes. Also we prove that the resonance structure converges to the allowed energy bands in the infinite size limit. In section 4, we obtain the Wigner time delay function and we discuss the effect of the resonances on this quantity. In section 5, we illustrate the results of sections 3 and 4 in simple systems. The conclusion and comments are given in section 6.

2. Scattering resonances

Let us consider the Schrödinger equation with the potential

$$V(x) = \begin{cases} 0 & \text{for} \quad x < -\frac{L}{2} \\ f(x) & \text{for} \quad -\frac{L}{2} < x < \frac{L}{2} \\ 0 & \text{for} \quad x > \frac{L}{2} \end{cases} \tag{1}$$

where $f(x)$ is a periodic function of spatial period a: $f(x+a) = f(x)$,which is prolongated by a vanishing potential outside the interval $-\frac{L}{2} < x < \frac{L}{2}$ with $L = an$.

Since the potential acts in a finite region, we are here concerned with a scattering system. In this regard, we notice that the energy spectrum of a scattering system is very different from the band structure of the infinite system with potential $f(x)$. For the present scattering system, the energy spectrum is continuous from zero to infinity with possible eigenenergies corresponding to the bound states.

However, such a scattering system also sustains decaying processes which are described in terms of resonances representing the metastable states of the scatterer.

Let us first briefly review the concept of resonance [1–4, 7]. In a scattering system, the Hamiltonian operator decomposes as $H = H_0 + V$ into a free motion part and the interaction potential. The scattering wavefunction at energy E can be obtained by inverting the Lippmann–Schwinger equation

$$|\psi_{Ec}^{\pm}\rangle = |\phi_{Ec}\rangle + G(E \pm \mathrm{i}0)V|\phi_{Ec}\rangle \tag{2}$$

where the states ϕ_{Ec} form a complete set of eigenfunctions of H_0, and where $G(z) = (z-H)^{-1}$ is called the resolvent of H. The scattering states (2) together with the bound states of the system form a complete basis [2]. It is known that the time evolution of a wavepacket can be decomposed on the bound states and the scattering states [2, 4].

Furthermore, the resolvent operator of H presents poles in a complex energy surface formed by two Riemann sheets joined together along a branch cut starting at zero kinetic energy

$E = 0$. On one hand, real poles corresponding to the bound states appear on the negative real-energy axis of the first Riemann sheet. On the other hand, complex poles corresponding to resonant states appear in the lower half of the second Riemann sheet [7]. The time evolution of a wavepacket can alternatively be expressed in terms of the resonance poles which contribute by exponential decays. In this alternative representation, the branch point at $E = 0$ contributes by a long-time tail term which may generally be neglected because this contribution is only important for particles emitted with a very slow velocity which is practically never the case. The time evolution of the amplitude to detect the wavepacket ψ_t in the state ϕ_d is thus

$$\langle \phi_d | \psi_t \rangle \approx \sum_r c_r \mathrm{e}^{-\frac{\mathrm{i}E_r}{\hbar}t} + \sum_B c_B \mathrm{e}^{-\frac{\mathrm{i}E_B}{\hbar}t} \tag{3}$$

with real and negative E_B and complex

$$E_r = \epsilon_r - \mathrm{i}\frac{\Gamma_r}{2}. \tag{4}$$

Γ_r is called the width of the resonance. If the detecting state ϕ_d or the prepared state ψ_0 have a negligible overlap with the bound states as in typical scattering processes, the experiment will only observe the superposition of exponential decays due to the resonances. In the case where a single resonance is excited we have that $|\psi_t\rangle \sim \mathrm{e}^{-\frac{\mathrm{i}E_r}{\hbar}t}$, and we see that the probability density decays as $|\psi_t|^2 \sim \mathrm{e}^{-\frac{\Gamma_r}{\hbar}t}$ so that the lifetime of the resonance can be inferred to be

$$\tau_r = \frac{\hbar}{\Gamma_r}. \tag{5}$$

When the asymptotic motion is a free plane wave, the energy is related to the wavenumber k by

$$E = \frac{\hbar^2 k^2}{2m}. \tag{6}$$

Each pole in the Riemann complex-energy surface corresponds to one pole in the complex wavenumber plane and vice versa according to

$$\epsilon_r = \frac{\hbar^2}{2m}(\mathrm{Re}\, {k_r}^2 - \mathrm{Im}\, {k_r}^2) \tag{7}$$

and

$$\Gamma_r = -\frac{2\hbar^2}{m}\,\mathrm{Re}\, k_r\, \mathrm{Im}\, k_r. \tag{8}$$

Due to the relation between the resolvent and the S-matrix, poles of the resolvent are also poles of the S-matrix [3]. Therefore, we can also compute resonances and bound-state energies from the S-matrix.

3. Resonances of periodic systems

3.1. The S-matrix

In this section we first obtain the S-matrix in order to calculate the spectrum of the scattering resonances for one-dimensional finite periodic systems. With this aim, we consider the one-dimensional stationary Schrödinger equation

$$-\frac{\hbar^2}{2m}\varphi''(x) + V(x)\varphi(x) = E\varphi(x) \tag{9}$$

with a potential $V(x)$ which is obtained by juxtaposing n 'unit cells' of length a as discussed in the introduction. The interaction region has a total length $L = an$.

The scattering problem is formulated with a method based on a transfer matrix associated with a 'unit cell' of the one-dimensional chain. Such a method has been developed by several authors [14, 15].

We call R_j the region $ja - a/2 < x < ja + a/2$, with $j = -(N-1), \ldots, N-1$. R_{-N} and R_N are the external regions, i.e. $x \in R_N$ if $x > (N-1)a + a/2$ and $x \in R_{-N}$ if $x < -(N-1)a - a/2$. In the exterior regions the solutions are

$$\varphi_k(x) = A_{-N}\mathrm{e}^{\mathrm{i}kx} + A'_{-N}\mathrm{e}^{-\mathrm{i}kx} \qquad x \in R_{-N} \tag{10}$$

and

$$\varphi_k(x) = A_N\mathrm{e}^{\mathrm{i}kx} + A'_N\mathrm{e}^{-\mathrm{i}kx} \qquad x \in R_N. \tag{11}$$

In the interior region R_j the solution is

$$\varphi_k(x) = A_j v_k(x - aj) + A'_j v'_k(x - aj) \qquad x \in R_j \tag{12}$$

where $v_k(x)$ (resp. $v'_k(x)$) is a solution of (9) with $V(x) = V_1(x)$, given by the potential in the unit cell and zero elsewhere, that matches smoothly with $\mathrm{e}^{\mathrm{i}kx}$ (resp. $\mathrm{e}^{-\mathrm{i}kx}$) at the left free region and with a linear combination $F(k)\mathrm{e}^{\mathrm{i}kx} + G(k)\mathrm{e}^{-\mathrm{i}kx}$ (resp. $F'(k)\mathrm{e}^{\mathrm{i}kx} + G'(k)\mathrm{e}^{-\mathrm{i}kx}$) at the right free region [14, 16]. The solution in the whole space is obtained by matching these various expressions for φ_k at $x = ja + a/2$ with $j = -N, \ldots, N-1$.

The procedure is as follows. Remove all but one (the jth) unit cell. For $x < ja - a/2$ we have

$$\varphi_k(x) = A_j\mathrm{e}^{\mathrm{i}k(x-aj)} + A'_j\mathrm{e}^{-\mathrm{i}k(x-aj)} \tag{13}$$

and for $x > ja + a/2$

$$\varphi_k(x) = \tilde{A}_j\mathrm{e}^{\mathrm{i}k(x-aj)} + \tilde{A}'_j\mathrm{e}^{-\mathrm{i}k(x-aj)}. \tag{14}$$

By the properties discussed for the $v_k(x)$ and $v'_k(x)$, we have that:

$$\tilde{A}_j = A_j F(k) + A'_j F'(k) \tag{15}$$

$$\tilde{A}'_j = A_j G(k) + A'_j G'(k). \tag{16}$$

For a real potential we have that if $\varphi_k(x)$ is a solution of (9) then $\varphi^*_k(x)$ is also a solution. This implies that

$$G'(k) = F^*(k) \tag{17}$$

$$F'(k) = G^*(k) \tag{18}$$

so

$$\begin{pmatrix} \tilde{A}_j \\ \tilde{A}'_j \end{pmatrix} = M(k) \begin{pmatrix} A_j \\ A'_j \end{pmatrix} \tag{19}$$

with

$$M = \begin{pmatrix} F(k) & G^*(k) \\ G(k) & F^*(k) \end{pmatrix} \tag{20}$$

which satisfies

$$\det M = 1 \tag{21}$$

as a consequence of the probability conservation. Defining the transmission and reflection probabilities for a 'unit cell' as

$$T_1 = \frac{1}{|F(k)|^2} \tag{22}$$

$$R_1 = \frac{|G(k)|^2}{|F(k)|^2} \tag{23}$$

equation (21) is equivalent to

$$T_1 + R_1 = 1. \tag{24}$$

Note that $0 \leqslant R_1 < 1$ and $0 < T_1 \leqslant 1$.

At the left-hand end of the jth cell the function $\varphi_k(x)$ defined in (12) has the same value and derivative as the superposition of plane waves (13). Similarly at the right-hand end of this cell it has the same value and derivative as (14). These results enable us to write simply the matching conditions in the periodic structure.

Noting that the right-hand end of the jth cell is the left-hand end of the $(j+1)$th cell, we have that $\tilde{A}_j e^{ik(x-aj)} + \tilde{A}'_j e^{-ik(x-aj)}$ has the same value and derivative as $A_{j+1}e^{ik(x-a(j+1))} + A'_{j+1}e^{-ik(x-a(j+1))}$, i.e.

$$\begin{pmatrix} A_{j+1} \\ A'_{j+1} \end{pmatrix} = D(k) \begin{pmatrix} \tilde{A}_j \\ \tilde{A}'_j \end{pmatrix} \tag{25}$$

with

$$D(k) = \begin{pmatrix} e^{ika} & 0 \\ 0 & e^{-ika} \end{pmatrix} \tag{26}$$

and so we get

$$\begin{pmatrix} A_{j+1} \\ A'_{j+1} \end{pmatrix} = D(k)M(k) \begin{pmatrix} A_j \\ A'_j \end{pmatrix}. \tag{27}$$

By iteration along the chain the whole solution is obtained in terms of two arbitrary constants A_{-N} and A'_{-N}. The coefficient of the two external regions R_{-N} and R_N are thus related by

$$\begin{pmatrix} A_N \\ A'_N \end{pmatrix} = \tilde{M}(k) \begin{pmatrix} A_{-N} \\ A'_{-N} \end{pmatrix} \tag{28}$$

where

$$\tilde{M}(k) = \begin{pmatrix} e^{-ikNa} & 0 \\ 0 & e^{ikNa} \end{pmatrix} Q^n \begin{pmatrix} e^{-ik(N-1)a} & 0 \\ 0 & e^{ik(N-1)a} \end{pmatrix} \tag{29}$$

with $n = 2N - 1$ (the number of cells) and

$$Q(k) = D(k)M(k) \tag{30}$$

is the iteration matrix [14]. The diagonal matrices in equation (29) are introduced in order to use the iteration matrix starting at the left-hand side with the wavefunction (10) and ending at the right-hand side with (11).

The S-matrix allows us to calculate the amplitude of the outgoing waves in terms of the amplitudes of the incoming waves, i.e.

$$\begin{pmatrix} A_N \\ A'_{-N} \end{pmatrix} = S(k) \begin{pmatrix} A_{-N} \\ A'_N \end{pmatrix}. \tag{31}$$

Using the fact that $\det \tilde{M}(k) = 1$ (probability conservation) we get from equation (28)

$$S(k) = \frac{1}{\tilde{M}_{22}} \begin{pmatrix} 1 & \tilde{M}_{12} \\ -\tilde{M}^*_{12} & 1 \end{pmatrix} \tag{32}$$

for S.

3.2. Diagonalization of Q and the infinite-system properties

In order to compute $\tilde{M}(k)$ and thus the S-matrix, we now turn to the diagonalization of $Q(k)$:

$$Q = P\lambda P^{-1} \tag{33}$$

with

$$P = \begin{pmatrix} Q_{12} & Q_{12} \\ \lambda_+ - Q_{11} & \lambda_- - Q_{11} \end{pmatrix} \tag{34}$$

and

$$\lambda = \begin{pmatrix} \lambda_+ & 0 \\ 0 & \lambda_- \end{pmatrix}. \tag{35}$$

The eigenvalues of Q are

$$\lambda_\pm = \mathrm{Re}\, Q_{11} \pm \sqrt{(\mathrm{Re}\, Q_{11})^2 - 1}. \tag{36}$$

As we will frequently refer to the infinite size limit we want to summarize the basic results concerning the infinite periodic system.

For an infinite periodic system the symmetry with respect to lattice translations implies the existence of energy bands. According to Bloch's theorem, the wavefunction satisfies

$$\phi(x + a) = \exp(\mathrm{i}qa)\phi(x) \tag{37}$$

and the eigenenergies $E_n(q)$ are labelled by the quasi-momentum or Bloch parameter q. This means that the iteration matrix (30) has eigenvalues (36) of unit modulus [14]

$$\lambda_\pm = \exp(\mathrm{i}qa) \tag{38}$$

a condition that is satisfied if

$$(\mathrm{Re}\, Q_{11})^2 - 1 < 0 \tag{39}$$

as we can see from equation (36). This condition gives the edges of the bands $k_b^\pm$ as solutions of

$$\mathrm{Re}\, Q_{11}(k_b^\pm) = \pm 1 \tag{40}$$

such that $|\mathrm{Re}\, Q_{11}(\mathrm{Re}\, k)| < 1$ for $k_b^\pm < \mathrm{Re}\, k < k_b^\mp$.

From equations (36) and (38) we see that the Bloch parameter q is related to k by

$$q(k) = \frac{1}{a} \arccos \mathrm{Re}\, Q_{11} \tag{41}$$

and to the energy by $E = \frac{\hbar^2 k^2}{2m}$. From equation (40) we see that the edges of the band correspond to $q = 0$ or $q = \frac{\pi}{a}$. Thus for an infinite periodic system the parameter q takes values in the interval $(0, \frac{\pi}{a})$ known as the first Brillouin zone. In this interval each energy band $E_n(q)$ is a univalued function of q. We notice that the connection between the scattering by a finite periodic potential and the Bloch parameter has already been discussed in the literature [15, 17]

3.3. The scattering resonances

According to (32), we can compute the poles of the S-matrix as zeros of $\tilde{M}_{22}$ which is the inverse of the total transmission amplitude, we call t_T^{-1} from now on.

From equations (33)–(35) and equation (29) we get

$$\tilde{M}_{22} = t_T^{-1} = \frac{\exp(\mathrm{i}kan)}{\lambda_+ - \lambda_-}[\lambda_+^n(\lambda_+ - Q_{11}) - \lambda_-^n(\lambda_- - Q_{11})]. \tag{42}$$

Let us recall that n is the number of cells. The resonances are the complex values of k that satisfy

$$\lambda_+^n(\lambda_+ - Q_{11}) = \lambda_-^n(\lambda_- - Q_{11}). \tag{43}$$

We will rewrite equations (42) and (43) for real values of k that belong to the intervals $k_b^{\pm} < \mathrm{Re}\, k < k_b^{\mp}$ and then prolongate it in the complex plane in order to find the resonances.

In those intervals we set

$$\lambda_\pm = \mathrm{e}^{\pm \mathrm{i} q(k) a} \tag{44}$$

where we introduce the function $q(k)$ given in (41) which corresponds to the Bloch parameter of the infinite system.

From equations (36) and (41)

$$\lambda_\pm - Q_{11} = -\mathrm{i}\,\mathrm{Im}\, Q_{11} \pm \mathrm{i} \sin qa. \tag{45}$$

We note that

$$\mathrm{Im}\, Q_{11} = \sqrt{|Q_{11}|^2 - (\mathrm{Re}\, Q_{11})^2} \tag{46}$$

and $|Q_{11}|^2$ is the inverse of the transmission probability T_1 for the unit cell so that we get

$$\mathrm{Im}\, Q_{11} = (\sin qa)\sqrt{1 + \frac{R_1}{T_1 \sin^2 qa}} \tag{47}$$

where we have used the relation $R_1 + T_1 = 1$. Equations (45) and (47) give

$$\lambda_\pm - Q_{11} = \mathrm{i}(\sin qa)\left(-\sqrt{1 + \frac{R_1}{T_1 \sin^2 qa}} \pm 1\right). \tag{48}$$

Replacing (48) and (44) in (42), we get the inverse of the total transmission coefficient as

$$t_T^{-1} = \exp(\mathrm{i}kan)\left(\cos qan - \mathrm{i}\sqrt{1 + \frac{R_1}{T_1 \sin^2 qa}} \sin qan\right). \tag{49}$$

We can write equation (43) using (48) and (41) and we finally obtain that the resonances satisfy

$$\mathrm{e}^{2\mathrm{i}qan} = \frac{2T_1 \sin^2 qa}{R_1}\left(1 + \sqrt{1 + \frac{R_1}{T_1 \sin^2 qa}} + \frac{R_1}{2T_1 \sin^2 qa}\right). \tag{50}$$

This equation is completely equivalent to (43) and it determines the resonances of the system after prolongation in the complex k-plane. The size of the system, the function q introduced in equation (41) and the reflection and transmission probabilities of the unit cell determine this spectrum and the total transmission coefficient as well. From equation (49) we can see that the total transmission probability is

$$T_T = |t_T|^2 = \frac{1}{1 + \frac{R_1 \sin^2 qan}{T_1 \sin^2 qa}}.$$

Accordingly, perfect transmission ($T_T = 1$) occurs whenever $R_1 = 0$ ($T_1 = 1$), or when $qan = m\pi$ for $m = 1, 2, \ldots, n-1$. Therefore, in the general case ($R_1 \neq 1$), the transmission probability has $n - 1$ peaks with $T_T = 1$ under each allowed energy band as q increases by $\frac{\pi}{a}$ [15]. Since the peaks in the transmission probability (or in general in the cross section) are associated with resonances we expect to find $n - 1$ resonances under each allowed energy band.

3.4. The asymptotic resonance band structure

In this section, we turn to an approximate description of this spectrum for high energies. In the domain of high energies, the reflection probability for one unit cell can be computed from perturbation theory [18] and gives:

$$R_1(k) \approx \frac{m^2}{\hbar^4 k^2}\left|\int_{-\infty}^{+\infty} V_1(x)\exp(2\mathrm{i}kx)\,\mathrm{d}x\right|^2. \tag{51}$$

As a consequence, we observe that this reflection probability decreases as $|k| \to \infty$. Hence, we can expand equation (50) in powers of R_1 which gives at the leading order

$$\mathrm{e}^{\mathrm{i}qan} \approx \pm\frac{2}{\sqrt{R_1(k)}}\sin qa \tag{52}$$

where the dependence on the wavenumber k appears in the reflection probability R_1. Now we will assume that $R_1(k) \approx R_1(\mathrm{Re}\,k)$. This condition is justified by the fact that we are interested in the leading resonances, which are the closest to the real axis, and that we assume R_1 to be a smooth function of k.

The function $q(k)$ takes complex values in the complex k-plane. We define

$$u = a\,\mathrm{Re}\,q(k) \tag{53}$$

$$v = a\,\mathrm{Im}\,q(k). \tag{54}$$

After introducing equations (53) and (54) into equation (52) we obtain, from the real and imaginary parts, two equations:

$$\exp(-nv)\cos un = \pm\frac{1}{\sqrt{R_1(\mathrm{Re}\,k)}}\sin u\cosh v \tag{55}$$

$$\exp(-nv)\sin un = \pm\frac{1}{\sqrt{R_1(\mathrm{Re}\,k)}}\cos u\sinh v. \tag{56}$$

Adding the squares of equations (55) and (56) we get for u

$$u = \arccos\left(\pm\sqrt{\cosh^2 v - \frac{R_1(\mathrm{Re}\,k)}{4}\exp(-2nv)}\right). \tag{57}$$

The signs $\pm$ come from the fact that u is a bivalued function of v in each interval $|\cosh^2 v - \frac{R_1}{4}\mathrm{e}^{-2nv}| < 1$. The leading resonances are points on this curve.

To plot the function (57) in the k-plane one has to consider the function $k = k(q)$ but, for the high-energy regime that we consider, we can use the results of perturbation theory of a weak periodic potential [13].

The zeroth-order approximation for $E_n(q)$ allows us to consider that $q = |k| \bmod(\frac{\pi}{a})$. The potential produces second-order corrections to the energy away from the band edges. At the band edges, when Bragg reflection occurs, the corrections are of first-order in the potential. Therefore, we can expect to have a good approximation to our curve considering $q = |k| \bmod(\frac{\pi}{a})$ except at the borders of the structure.

Substituting this approximation in equation (57), we finally obtain the following approximate expression for the pattern of resonances in one-dimensional periodic systems:

$$\cos^2 a\,\mathrm{Re}\,k = \cosh^2 a\,\mathrm{Im}\,k - \frac{R_1(\mathrm{Re}\,k)}{4}\exp(-2na\,\mathrm{Im}\,k). \tag{58}$$

The implicit function $\mathrm{Re}\,k = \mathrm{Re}\,k(\mathrm{Im}\,k)$ defined by equation (58) gives the structure that the scattering resonances display in the complex wavenumber k-plane in the high-energy regime.

We restrict ourselves to the case that R_1 is an almost constant function of $\operatorname{Re} k$ in intervals of the order $\Delta k \approx \frac{\pi}{a}$. In this case, we can write the explicit function

$$a \operatorname{Re} k = \arccos\left(\pm\sqrt{\cosh^2 a \operatorname{Im} k - \frac{R_1}{4}\exp(-2na \operatorname{Im} k)}\right) \pmod{\pi}. \quad (59)$$

Our aim is now to obtain the upper and lower envelopes of the resonance structure. The study of these envelopes give us the dependence of this structure on the size of the system. A very good expression for the lower envelope can be obtained by evaluating equation (59) at the value $a \operatorname{Re} k = \frac{\pi}{2} \pmod{\pi}$ which corresponds to the minimum of the curve (see figure 2 of section 5). We obtain

$$\frac{2}{\sqrt{R_1}} = \frac{\exp(-L \operatorname{Im} k_{inf})}{\cosh a \operatorname{Im} k_{inf}}. \quad (60)$$

On the other hand, an approximation for the upper envelope is given by evaluating equation (59) at $a \operatorname{Re} k = 0 \pmod{\pi}$ which corresponds to a maximum (see figure 2).

$$\frac{2}{\sqrt{R_1}} = \frac{\exp(-L \operatorname{Im} k_{sup})}{|\sinh a \operatorname{Im} k_{sup}|}. \quad (61)$$

We note that in the previous results (60) and (61), no assumption has been made with respect to the size L.

According to the aforementioned assumption that R_1 is an almost constant over $\Delta k \approx \frac{\pi}{a}$, $\frac{2}{\sqrt{R_1}}$ is a smooth and increasing function of $\operatorname{Re} k$ and after inversion we get the upper and lower envelopes. Moreover an expression of $\operatorname{Im} k$ in terms of $\operatorname{Re} k$ is physically desirable because $\operatorname{Re} k$ is directly related to the band. This kind of expression can be obtained for sufficiently large values of n and $\operatorname{Re} k$. We finally obtain

$$\operatorname{Im} k_{inf} \approx -\frac{1}{L}\ln\left[\frac{2}{\sqrt{R_1(\operatorname{Re} k)}}\right] \quad (62)$$

$$\operatorname{Im} k_{sup} \approx -\frac{1}{L}\ln\left[\frac{2}{\sqrt{R_1(\operatorname{Re} k)}}\frac{a}{L}\left|\ln\left[\frac{2}{\sqrt{R_1(\operatorname{Re} k)}}\right]\right|\right]. \quad (63)$$

Equation (63) holds under the condition $\ln(\frac{2}{\sqrt{R_1}}) \sim L$, which is consistent with the high-energy domain that we consider.

We see from equation (62) that the imaginary parts of the leading resonances vanish $\operatorname{Im} k \to 0$ for $L \to \infty$. Therefore, in the limit $L \to \infty$ we have that

$$u = a \operatorname{Re} q(\operatorname{Re} k + \mathrm{i} \operatorname{Im} k) \to a \operatorname{Re} q(\operatorname{Re} k) \quad (64)$$

$$v = a \operatorname{Im} q(\operatorname{Re} k + \mathrm{i} \operatorname{Im} k) \to a \operatorname{Im} q(\operatorname{Re} k). \quad (65)$$

The function $q(\operatorname{Re} k)$ is pure real in intervals of $\operatorname{Re} k$ corresponding to the allowed energy bands where it satisfies $0 < q(\operatorname{Re} k) < \frac{\pi}{a}$ or pure imaginary in the forbidden bands as can be seen from equations (36) and (44). From equation (57) we have that $0 < u < \frac{\pi}{a}$ which, in the limit that we consider, means that $0 < \operatorname{Re} q(\operatorname{Re} k) < \frac{\pi}{a}$ which implies that $k_b^+ < \operatorname{Re} k < k_b^-$. Since the function $q(\operatorname{Re} k)$ determines the energy band of the infinite system while the functions $u(k)$ and $v(k)$ determine the scattering resonances, we have proved that the leading resonances converge to the allowed energy bands in the infinite-system limit $L \to \infty$.

In fact, the function (59) gives the curve of the leading resonances under the band where $R_1(\operatorname{Re} k)$ takes the almost constant value R_1. This small-scale structure appears below every interval of $\operatorname{Re} k$ which corresponds to an allowed energy band with possible variations only due to the slow dependence of $R_1(\operatorname{Re} k)$ in this interval. On the other hand, long-scale variations in the resonance structure are determined by the lower and upper envelopes, (62) and (63).

3.5. The asymptotic resonance widths

From equations (59) and (8), we can now obtain the values for the decay rates of the leading resonances in each band. For the high-energy domain $\ln(\frac{2}{\sqrt{R_1}}) \sim L$, we get the following expressions for the decay rate of the resonances located below a band in the corresponding infinite system:

$$\Gamma(\mathrm{Re}\,k) \approx \frac{2\hbar^2}{m}(\mathrm{Re}\,k)\frac{1}{L}\ln\left[\frac{2}{\sqrt{R_1}}\sin(a\,\mathrm{Re}\,k)\right]. \tag{66}$$

This approximation is valid in the bulk of the band but it fails near the edges of the energy bands where an approximate value for the width is then given by the upper envelope calculated in equation (63)

$$\Gamma(\mathrm{Re}\,k) \approx \frac{2\hbar^2}{m}(\mathrm{Re}\,k)\frac{1}{L}\ln\left[\frac{2}{\sqrt{R_1}}\frac{a}{L}\ln\left(\frac{2}{\sqrt{R_1}}\right)\right]. \tag{67}$$

Therefore in the limit $L \to \infty$ the width of each resonance is inversely proportional to the size of the system. From equations (66) and (67) we observe that the widths of the resonances near the edges of the resonance structure are smaller than the width of the resonances in the bulk giving a lengthening in the lifetimes of the resonances at the edges of the resonance bands. This lengthening appears also in the Wigner time delay function.

4. Wigner's time delay

4.1. Connection to the S-matrix

The time delay was introduced by Wigner [5] in the case of a single channel scattering and later extended to many channels by Smith [6]. Wigner's derivation uses a wavepacket analysis with packets of arbitrarily small energy width. The time delay is defined from the phase difference between the peak of the scattered wave and the peak of a freely propagating one [4]. In the approach given by Smith, the time delay is the ratio of the excess number of particles due to the interaction to the incident flux. Smith's analysis is based on stationary states of the systems with fixed energy. He constructs a matrix O where each diagonal element O_{ii} corresponds to the average time delay of an incident particle in the i-channel, where the average is made with the probability that the outgoing particle is in a j-channel for all j. The trace of this matrix is the sum of the time delay of all the channels. Thus for a finite number of channels (as in our case) the total average time delay can be expressed as the trace of O over the number of channels. Considering the explicit expression of O in terms of the S-matrix and the fact that in our problem there are two channels, the average time delay is

$$\tau(E) = -\frac{\mathrm{i}\hbar}{2}\,\mathrm{tr}\,\frac{\mathrm{d}}{\mathrm{d}E}\ln S(E) = -\frac{\mathrm{i}\hbar}{2}\frac{\mathrm{d}}{\mathrm{d}E}\ln\det S(E). \tag{68}$$

In the case of a single channel we recover from this equation Wigner's result.

It is convenient to define a interaction time $T_{int}(E)$ by the relation

$$\tau(E) = T_{int}(E) - T_{free}(E) \tag{69}$$

where

$$T_{free}(E) = \frac{L}{v_{free}} \tag{70}$$

is the time of a free flight at the velocity $v_{free} = \frac{\hbar k}{m}$.

Using the results of section 3, equation (68) can be written as

$$\tau(E) = -\overline{h}\,\mathrm{Im}\,\frac{\mathrm{d}}{\mathrm{d}E}\ln t_T^{-1}. \tag{71}$$

From (42) we have

$$\ln t_T^{-1} = \ln\left[\frac{\lambda_+^n(\lambda_+ - Q_{11}) - \lambda_-^n(\lambda_- - Q_{11})}{(\lambda_+ - \lambda_-)}\right] + \mathrm{i}kan. \tag{72}$$

The term ikan gives the time of free propagation. In fact, this contribution is obtained by

$$-\overline{h}\,\mathrm{Im}\,\frac{\mathrm{d}}{\mathrm{d}E}(\mathrm{i}kan) = -\frac{Lm}{\overline{h}k} = -\frac{L}{v_{free}} = -T_{free}. \tag{73}$$

The other term in equation (72) gives the interaction time. As we shall see, the behaviour of this quantity is very different for energies in the allowed or in the forbidden regions.

4.2. Behaviour of the interaction time in the forbidden energy regions

In the forbidden regions, λ_+ and λ_- are real numbers and can be written as $\lambda_\pm = \exp(\pm\kappa a)$. If we write the term inside the square bracket in equation (72) in the polar form $\rho\exp(\mathrm{i}\theta)$, the imaginary part of the logarithm gives θ so $T_{int} = -\overline{h}\frac{\mathrm{d}\theta}{\mathrm{d}E}$. Using

$$\lambda_\pm - Q_{11} = -\mathrm{i}\,\mathrm{Im}\,Q_{11} \pm \sqrt{(\mathrm{Re}\,Q_{11})^2 - 1} \tag{74}$$

we get

$$\theta = -\arctan\left[\frac{\mathrm{Im}\,Q_{11}}{\sqrt{(\mathrm{Re}\,Q_{11})^2 - 1}}\frac{\lambda_+^n - \lambda_-^n}{\lambda_+^n + \lambda_-^n}\right]. \tag{75}$$

The last factor is simply $\tanh an\kappa$ and we finally obtain

$$\theta = -\arctan\left[\frac{\mathrm{Im}\,Q_{11}}{\sqrt{(\mathrm{Re}\,Q_{11})^2 - 1}}\tanh an\kappa\right]. \tag{76}$$

Considering that $Q_{11} = \frac{1}{\sqrt{T_1}}\exp(\mathrm{i}\phi)$ we found that the interaction time in the forbidden regions is

$$T_{int}(E) = \overline{h}\frac{\cos^2\phi - T_1}{\cos^2\phi + \sin^2\phi\tanh^2 an\kappa - T_1}\frac{\mathrm{d}}{\mathrm{d}E}\frac{\sin\phi}{\sqrt{\cos^2\phi - T_1}}\tanh an\kappa. \tag{77}$$

One can interpret κ as the inverse of the evanescence length of the wavefunctions in the interaction region when the energy of the incident particle is in a forbidden band. The characteristic evanescence length l of this decay is $l \sim \frac{1}{\kappa}$. When $L = an > l$, $\tanh(L\kappa) \sim 1$ and $T_{int}(E)$ is size independent.

When $L = an < l$, $\tanh(L\kappa) \sim L\kappa$ and $T_{int}(E)$ depends almost linearly on the system size.

4.3. Behaviour of the interaction time in the allowed energy bands

To compute the interaction time in the allowed energy regions we rewrite the logarithmic term in a more convenient form:

$$T_{int}(E) = -\overline{h}\,\mathrm{Im}\,\frac{\mathrm{d}}{\mathrm{d}E}\left\{\ln\left[\lambda_-^n\frac{(\lambda_- - Q_{11})}{(\lambda_- - \lambda_+)}\left(1 - \lambda_+^{2n}\frac{(\lambda_+ - Q_{11})}{(\lambda_- - Q_{11})}\right)\right]\right\}. \tag{78}$$

The quotient $\frac{(\lambda_- - Q_{11})}{(\lambda_- - \lambda_+)}$ is real and positive as can be seen from equations (48) and (44) and do not contribute to the interaction time. The quotient $\frac{(\lambda_+ - Q_{11})}{(\lambda_- - Q_{11})}$ is real and of absolute value less than one. Using equation (44) we have for the interaction time

$$T_{int}(E) = -\hbar \frac{\mathrm{d}}{\mathrm{d}E} \left\{ -qan + \mathrm{Im}\ln\left[1 - \lambda_+^{2n} \frac{(\lambda_+ - Q_{11})}{(\lambda_- - Q_{11})}\right]\right\}. \tag{79}$$

The last term oscillates around zero and has peaks for each resonance. Resonances are also singularities in the complex k-plane of the time delay. The density of resonances decreases near the edges of the resonance structure and produces in the time delay the effects of isolated resonances. In the middle of the band the resonances overlap and give a small and smooth oscillatory contribution to the time delay. The first term gives the mean value of the interaction time in the allowed regions. Considering the fact that the velocity of a Bloch quasi-particle is $v_b = \frac{1}{\hbar}\frac{\mathrm{d}E}{\mathrm{d}q}$, the interaction time for the allowed energies is

$$T_{int} = \frac{L}{v_b} + t_{fl} \tag{80}$$

where t_{fl} is the contribution of the fluctuating part.

Generically, near the edges of the energy bands $v_b << 1$, then the interaction time is longer for energies near the edges of the allowed energy bands.

4.4. Behaviour of the interaction time in large systems

For large systems the *transmission* probability approaches the unit value in the allowed region so that we can identify the interaction time with the time of propagation in the interaction region. This is confirmed by equation (80) considering that, in the infinite system, the propagation is carried out exactly with the velocity v_b. On the other hand, in the forbidden regions, the *reflection* probability approaches the unit value so that the interaction time in that region should be interpreted as the time to be reflected. Intuitively, a reflected particle does not explore the complete system so it is not surprising that this time is size independent. We want to emphasize that no approximation has been made in this section. The system size, the energy and the shape of the potential in the unit cell are arbitrary, but for small systems when $L \to 0$, the oscillatory term t_{fl} is dominant and $\frac{L}{v_b}$ is no longer the average value of equation (80).

5. Applications to simple models

5.1. The finite Kronig–Penney model

We consider the potential

$$V(x) = V_0 \sum_{j=-N}^{N} \delta(x - aj). \tag{81}$$

The total transmission probability of this system has been studied in detail [15, 19].

We are here interested in the dynamical properties as characterized by the scattering resonances and the Wigner time delay. Figure 1 depicts a part of the wavenumber complex plane with the resonances for $n = 50$ and a zoom on the leading resonances for $n = 100$ for this system, where $n = 2N + 1$ is the total number of barriers.

We notice that equation (81) is the potential of the Kronig–Penney model in the limit $N \to \infty$. In this case the Bloch parameter q is related to the wavenumber k by

$$\cos qa = \cos ka + \frac{\alpha}{k} \sin ka \tag{82}$$

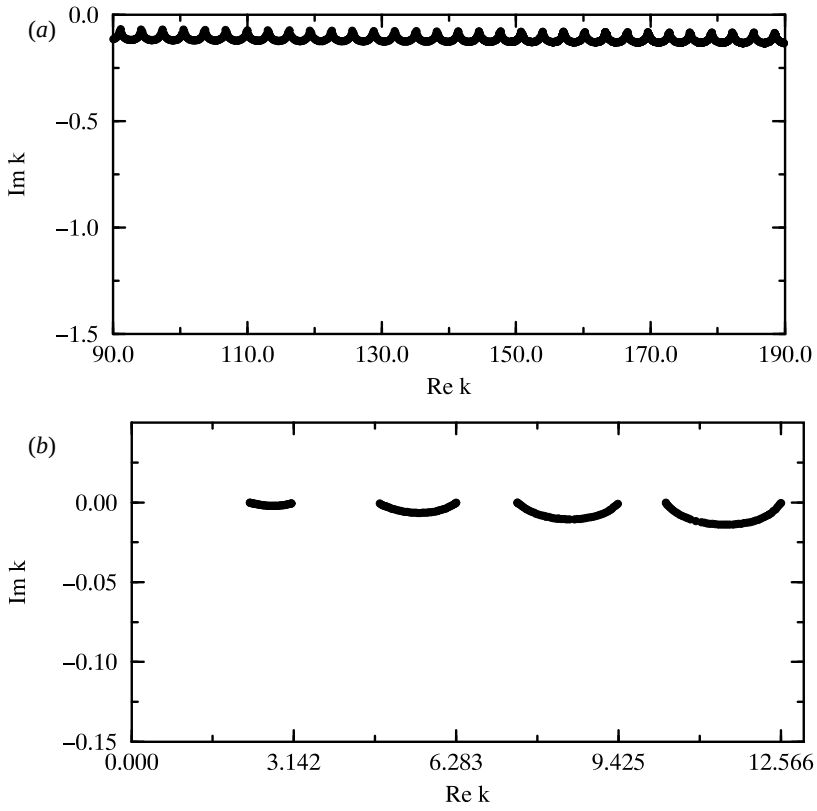

Figure 1. (*a*) The resonances of the finite Kronig–Penney model with $n = 50$ unit cells in a part of the complex wavenumber k-plane. (*b*) Zoom on the leading resonances at small $\mathrm{Re}\,k$ for $n = 100$. The resonances are below the bands of the Kronig–Penney model. Here, we have taken $\alpha = a = 1$.

where $\alpha = \frac{mV_0}{\hbar^2}$.

The reflection probability for a single barrier is

$$R_1 = \frac{\alpha^2}{k^2 + \alpha^2}. \tag{83}$$

For large k we have

$$R_1 = \frac{\alpha^2}{k^2} \tag{84}$$

which coincides with the result obtained using equation (51). Here R_1 is a smooth varying function of k, as we assumed in section 3. If V_0 is positive the allowed bands end at values of the wavenumber k which are multiples of $\frac{\pi}{a}$. To obtain the value of R_1 that characterizes the band we evaluate R_1 at $k = \frac{p\pi}{a}$. The predicted curve of resonances under the pth band is

$$\mathrm{Re}\,k - \frac{\pi p}{a} = \frac{1}{a}\arccos\left[\pm\sqrt{\cosh^2 a\,\mathrm{Im}\,k - \frac{\alpha^2}{4}\frac{a^2}{(p\pi)^2}\exp(-2an\,\mathrm{Im}\,k)}\right]. \tag{85}$$

In figure 2 we observe the nice fit of this curve with the resonances of the corresponding interval for the Kronig–Penney model.

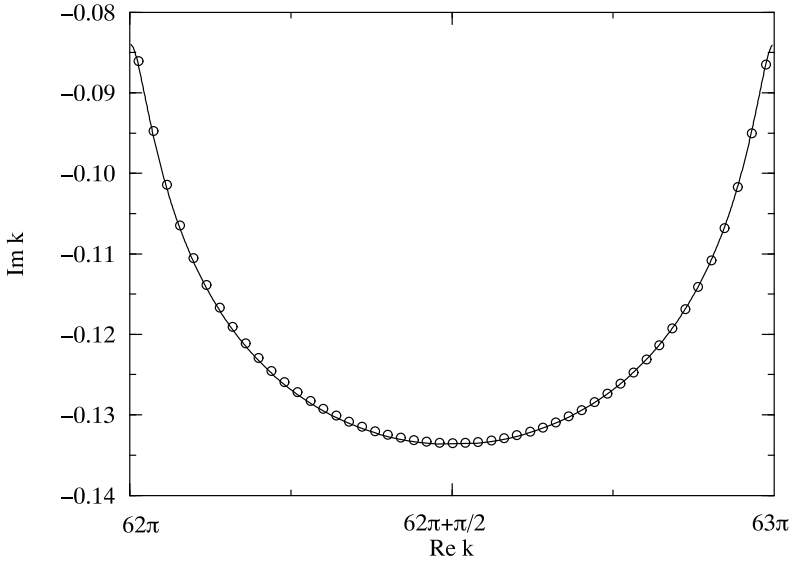

Figure 2. Resonances of the Kronig–Penney model composed of $n = 50$ cells. The resonances are plotted in the interval $(p-1)\pi < \mathrm{Re}\,k < p\pi$ with $p = 63$ together with the inverse function of (85). Here also $\alpha = a = 1$. We can here clearly observe that the number of resonances below the band is $n-1$. They are associated to the $n-1$ peaks in the transmission probability.

The envelopes obtained from equations (60) and (61)

$$\mathrm{Re}\,k|_{inf} = \frac{\alpha}{2}\frac{\exp -L\,\mathrm{Im}\,k}{\cosh a\,\mathrm{Im}\,k} \tag{86}$$

$$\mathrm{Re}\,k|_{sup} = \frac{\alpha}{2}\frac{\exp -L\,\mathrm{Im}\,k}{|\sinh a\,\mathrm{Im}\,k|} \tag{87}$$

are depicted in figure 3 together with the resonances, which confirms the global behaviour of the resonance spectrum predicted by our asymptotic theory.

For this system we have also computed the interaction time $T_{int}(E)$. Figure 4 depicts $T_{int}(E)$ together with the smooth term in equation (80) and the interaction time obtained by equation (77) in the limit of large systems. The figure clearly shows the lengthening of the Wigner time delay near the edges of the band predicted by equation (80).

The linear dependence on the system size in the allowed energy regions and the independence with respect to the size in the forbidden bands for large systems is shown in figure 5 which depicts the Wigner time delay for two chains of different sizes.

5.2. Finite sequence of potential barriers

Here the potential in the unit cell is given by

$$V_1(x) = \begin{cases} 0 & \text{for} \quad -\frac{a}{2} < x < -\frac{l}{2} \\ V_0 & \text{for} \quad -\frac{l}{2} < x < \frac{l}{2} \\ 0 & \text{for} \quad \frac{l}{2} < x < \frac{a}{2}. \end{cases} \tag{88}$$

We notice that the total transmission probability for the finite sequence of barriers have been analysed in [15, 19]. The Bloch parameter q of the infinite system and the wavenumber k are

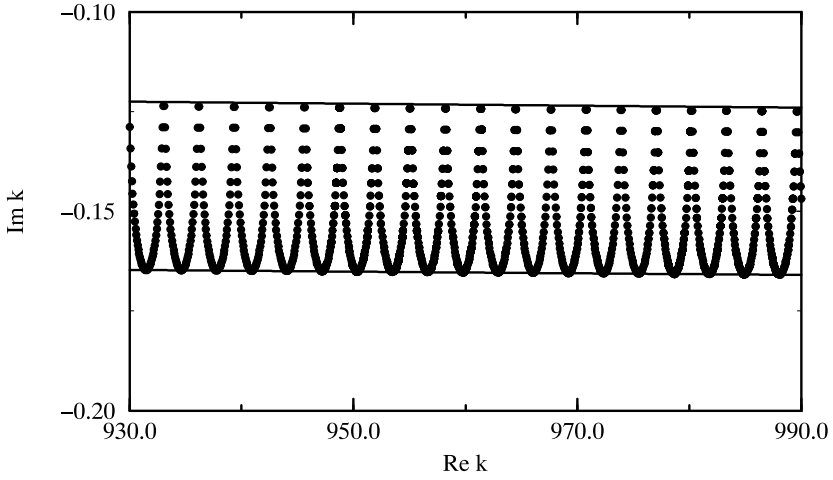

Figure 3. Resonances of the Kronig–Penney model composed of $n = 50$ unit cells with $\alpha = 1$ for large values of $\mathrm{Re}\, k$, with the envelopes given by (86) and (87).

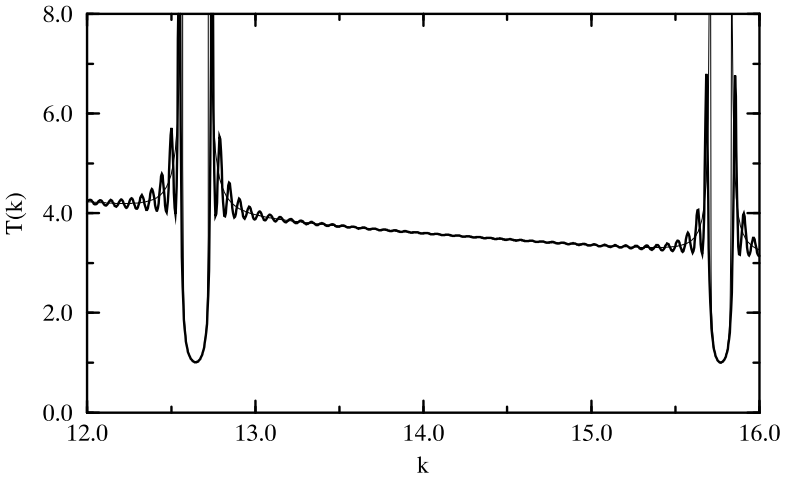

Figure 4. Interaction time $T_{int}(E)$ computed numerically from the Wigner time delay function for the Kronig–Penney model with $n = 50$ and $\alpha = 1$ (heavy curve). In the allowed energy regions, the smooth (light) curve is $\langle T_{int}(E)\rangle = \frac{L}{v_b}$ as given by equation (80). In the forbidden regions, the exact curve almost coincides with the approximation (light curve) obtained for large systems by equation (77).

related by

$$\cos qa = \cos k'l \cos k(a-l) - \frac{k^2 + k'^2}{2kk'} \sin k'l \sin k(a-l) \tag{89}$$

with $k' = \sqrt{k^2 - k_0^2}$ and $k_0 = \sqrt{\frac{2mV_0}{\hbar^2}}$. The reflection probability is

$$R_1 = \frac{k_0^4 \sin^2 k'l}{4k^2k'^2(\cos^2 k'l + \frac{(k^2+k'^2)^2}{4k^2k'^2} \sin^2 k'l)}. \tag{90}$$

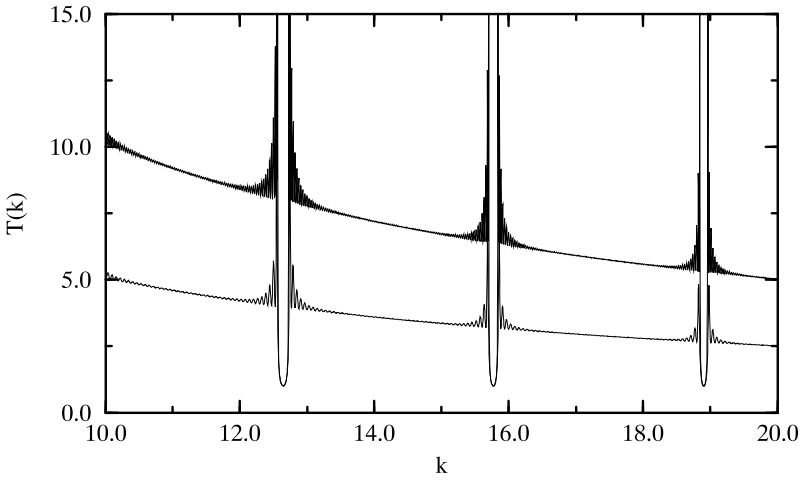

Figure 5. For $n = 50$ and $n = 100$, interaction time $T_{int}(E)$ of the Kronig–Penney model with $\alpha = 1$. This figure clearly shows that the interaction time is proportional to the length L in the allowed energy bands and that it is independent of L in the forbidden energy regions.

When $k' \to k$, this reflection probability tends to the value predicted by equation (51):

$$R_1 = \frac{k_0^4 \sin^2 kl}{4k^4}. \tag{91}$$

Accordingly, we observe that the reflection probability has variations in an interval $\Delta k = \frac{\pi}{l}$, which is larger than the approximate size $\frac{\pi}{a}$ of the allowed energy bands.

When $\frac{\pi}{l} \gg \frac{\pi}{a}$, R_1 can be considered as an almost constant function in most intervals of the order $\frac{\pi}{a}$. In this case, the resonances under the intervals of $\mathrm{Re}\, k$ corresponding to the allowed energy regions are given by the expression in equation (59) and the envelopes are given by equations (62) and (63), which gives the large-scale structure of the resonances for wavelength scales of the order $\frac{\pi}{l}$. This case is illustrated in figure 6 where $a = 1$ and $l = 0.0971$. Note that R_1 has zeros at $\mathrm{Re}\, k = \frac{n\pi}{l}$ where the envelopes diverge.

When $\frac{\pi}{l}$ is of the same order as $\frac{\pi}{a}$, we cannot consider R_1 to be an almost constant function in the energy band region and the analysis done after equation (58) is not strictly applicable. As an example, we consider $l = 1$ and $a = \frac{1+\sqrt{5}}{2}$. The resonances are plotted in figure 7. We can see that the resonances form a quasiperiodic structure in this case. We can interpret this structure as follows by using our results. The envelopes (62) and (63) of the structure here vary with a wavelength scale given by $\frac{\pi}{l}$ which is incommensurate with the wavelength scale $\frac{\pi}{a}$ of the band structure of the infinite system. This incommensurability creates the observed irregular behaviour.

6. Conclusion and comments

In this paper, we have studied in detail the resonance spectrum of a periodic scattering system. We have shown that this spectrum presents remarkable structures for which we have obtained an analytic expression at large energies. We have proved that the spectrum of scattering resonances presents a kind of band structure which converges to the allowed energy bands of the infinite periodic system in the limit of an infinite scatterer. This study shows that the widths of the resonances slowly increase with their energy and decreases like the inverse power of

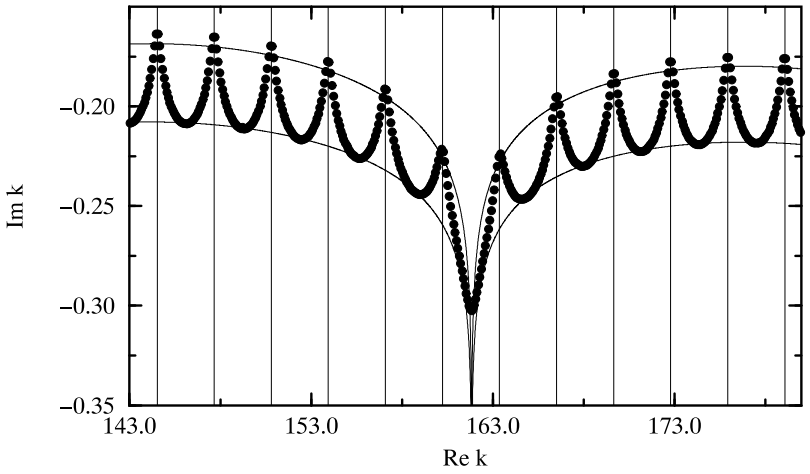

Figure 6. Resonances of a periodic potential composed of $n = 40$ unit cells as given by equation (88) with $a = 1$ and $l = 0.0971$ and $k_0 = \sqrt{\frac{2}{l}}$. The solid curves are the envelopes obtained with equations (62) and (63). The vertical lines indicate the forbidden regions which are very thin in this energy regime.

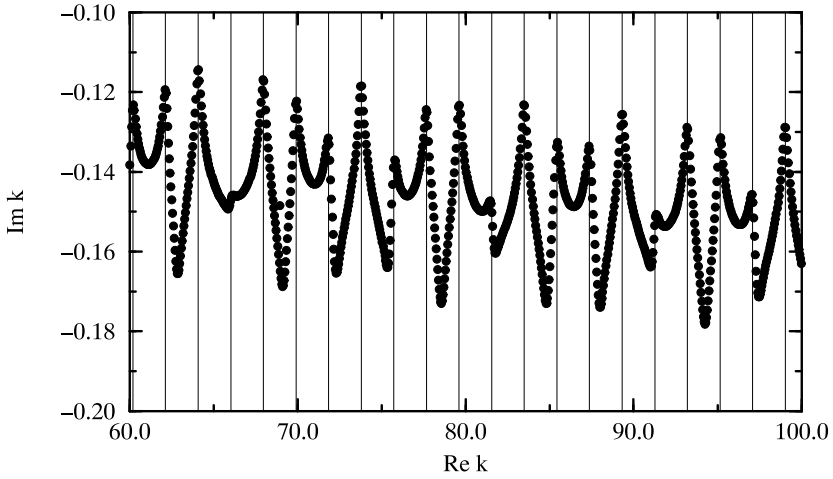

Figure 7. Resonances of a periodic potential composed of $n = 40$ unit cells as given by equation (88) with $a = \frac{1+\sqrt{5}}{2}$ and $l = 1$. The vertical lines indicate the forbidden regions which are very thin in this energy regime.

the size giving lifetimes proportional to the size of the system. This result is confirmed by the interaction time obtained in equation (80).

In systems where the reflection probability changes slowly with the wavenumber, we have shown that we should expect $n - 1$ resonances just below each allowed energy band in a finite system composed of n unit cells. Moreover, the metastable states with energies near the edges of the energy bands have longer lifetimes than the metastable states with energies in the bulk of the bands: see equations (59), (66) and (67). This can be understood as an effect of the slow propagation velocity $v_b = \frac{1}{\hbar}\frac{\mathrm{d}E}{\mathrm{d}q}$ of Bloch quasi-particles with energies near the edges of the bands in the corresponding infinite system. This fact is expressed for finite systems by the

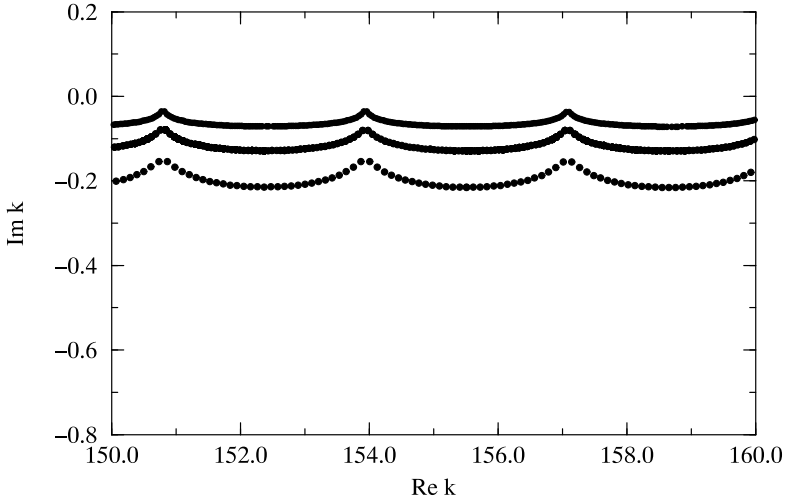

Figure 8. Resonances of the Kronig–Penney potential in equation (81) for $n = 30, 50, 90$ unit cells. We observe the convergence of the resonance spectrum toward the band structure on the real wavenumber axis when $L \to \infty$.

increase of the interaction time given by equation (80).

We have also shown that the resonance structure may become irregular already for certain one-dimensional systems characterized by two incommensurate lengths. In this case, our analysis provides the asymptotic behaviour of the domains of complex wavenumbers where the resonance spectrum fluctuates.

Our study leads up to the following general comments on the properties of scattering resonances in spatially extended systems:

(1) As we have mentioned before, the energy spectrum of the scattering system composed of a finite number n of cells is continuous on the real positive energy axis. However, these continuous energies correspond to waves scattered in the system from outside, whereas the internal and decay dynamics is controlled by the resonance spectrum. As the system becomes infinite ($n \to \infty$), the potential fills the whole space and the scattering from outside is no longer possible. Therefore, the aforementioned continuous spectrum no longer appears in the description of the infinite system. On the other hand, the resonance spectrum remains essentially determined by the internal dynamics when the system becomes spatially extended. In the same limit ($n \to \infty$), we can thus understand that it is precisely the resonance spectrum which converges to the spectrum of energy bands. Indeed, our results show that the number of resonances increases indefinitely (because the number of resonances is $n - 1$ inside each band as seen in figure 2) while they accumulate on the real energy-axis because their lifetime becomes infinite (see figure 8).

The above picture of the evolution of the resonances (or generalized spectrum [7]) is valid for unit cell potentials with well or barrier shapes. A potential composed of barriers can be transformed, by adding a constant energy potential in the exterior region, into a potential composed of wells. Obviously, both potentials have a band structure in the limit $n \to \infty$. Nevertheless, in textbooks of quantum mechanics, the second case is most often considered because it allows bound states so that the formation of the bands can be understood as an accumulation of the discrete energy eigenvalues of these bounds states in some intervals in the infinite-system limit. Here, we have presented the complementary scheme in which the band

structure is generated by the scattering resonances.

(2) We have here considered an ideal coupling to the external regions. One can consider more general couplings by multiplying the matrix $\tilde{M}$ at the left-hand side and at the right-hand side by another matrix M representing, for instance, two barriers. For large systems this will modify the resonance curve by a term proportional to the square root of the reflection probabilities of the new barriers (assumed to be small) and inversely proportional to the system size.

(3) Finally, concerning the time delay and its identification with a transmission time in the allowed energy regions, we would like to mention that several propositions for a traversal time exist in the literature. In fact the problem to get a suitable definition for such a quantity is not completely solved and the most common approaches have been critically reviewed by Landauer and Martin [20].

Acknowledgments

We would like to thank Professor G Nicolis for support and interest in this research and Dr D Alonso for help at the beginning of this work. FB is financially supported by a grant from the 'Communauté française de Belgique' and PG by the National Fund for Scientific Research (FNRS Belgium). This research has been supported in part by the Belgian government under 'Poles d'Attraction Interuniversitaires' programme, by the 'Quantum Keys for Reactivity' ARC project of the 'Communauté française de Belgique' and by the project 'Chaos and Quantum Mechanics in Mesoscopic Systems' of the 'Banque Nationale de Belgique'.

References

[1] Feshbach H 1958 *Ann. Phys.* **5** 357
Feshbach H 1962 *Ann. Phys.* **19** 287
[2] Joachain C J 1975 *Quantum Collision Theory* (Amsterdam: North-Holland)
[3] Gaspard P 1993 *Quantum Chaos* ed G Casati, I Guarneri and U Smilansky (Amsterdam: North-Holland) p 307
[4] Goldberger M L and Watson K M 1964 *Collision Theory* (New York: Wiley)
[5] Wigner E P 1955 *Phys. Rev.* **98** 145
[6] Smith F T 1960 *Phys. Rev.* **118** 349
[7] Böhm A 1979 *Quantum Mechanics* (New York: Springer)
[8] Gaspard P, Alonso D, Okuda T and Nakamura K 1994 *Phys. Rev.* E **50** 2591
[9] Burghardt I and Gaspard P 1997 *Chem. Phys.* **225** 259
[10] Schinke R, Keller H-M, Flöthmann H, Stumpf M, Beck C, Mordaunt D H and Dobbyn A J 1997 *Adv. Chem. Phys.* **101** 745
[11] Blümel R and Smilansky U 1988 *Phys. Rev. Lett.* **60** 477
[12] Šeba P 1991 *Phys. Rev.* A **43** 2068
[13] Ashcroft N W and Mermin N D 1976 *Solid State Physics* (Philadelphia, PA: Saunders)
[14] Cohen-Tannoudji C, Diu B and Laloë F 1977 *Quantum Mechanics* (New York: Wiley)
[15] Sprung D W L, Wu H and Martorell J 1993 *Am. J. Phys.* **61** 1118
[16] Arnold V I 1987 *Geometric Methods in the Theory of Ordinary Differential Equations* (Berlin: Springer)
[17] Newton R 1994 *Am. J. Phys.* **62** 1042
[18] Landau L and Lifshitz E 1965 *Quantum Mechanics, Nonrelativistic Theory* (Oxford: Pergamon)
[19] Rorres C 1974 *SIAM J. Appl. Math.* **27** 303
[20] Landauer R and Martin Th 1994 *Rev. Mod. Phys.* **66** 217